Rail accident analysis using large-scale investigations of train derailments on switches and crossings: comparing the performances of a novel stochastic mathematical prediction and various assumptions

Dindar, Serdar; Kaewunruen, Sakdirat; An, Min

DOI:
10.1016/j.engfailanal.2019.04.010

Document Version
Peer reviewed version

Citation for published version (Harvard):
Dindar, S, Kaewunruen, S & An, M 2019, 'Rail accident analysis using large-scale investigations of train derailments on switches and crossings: comparing the performances of a novel stochastic mathematical prediction and various assumptions', *Engineering Failure Analysis*, vol. 103, pp. 203-216. https://doi.org/10.1016/j.engfailanal.2019.04.010

Rail Accident Analysis using Large-Scale Investigations of Train Derailments on Switches and Crossings: Comparing the Performances of a Novel Stochastic Mathematical Prediction and Various Assumptions

Serdar Dindar, Sakdirat Kaewunruen, Min An

Keywords: Derailment, Turnout component failures, Hierarchical Bayesian analysis, Freight transportation, Spatial analysis

1 ABSTRACT

Each day tens of turnout-related derailment occur across the world. Not only is the prediction of them quite complex and difficult, but this also requires a comprehensive range of applications, and managing a well-designed geographic information system. With the advent of Geographic Information Systems (GIS), and computers-aided solutions, the last two decades have witnessed considerable advances in the field of derailment prediction. Mathematical models with many assumptions and simulations based on fixed algorithms were also introduced to estimate derailment rates. While the former requires a costly investment of time and energy to try and find the most fitting mathematical solution, the latter is sometimes a high hurdle for analysists since the availability and accessibility of geospatial data are limited, in general. As train safety and risk analysis rely on accurate assessment of derailment likelihood, a guide for transportation research is needed to show how each technique can approximate the number of observed derailments. In this study, a new stochastic mathematical prediction model has been established on the basis of a hierarchical Bayesian model (HBM), which can better address unique exposure indicators in segmented large-scale regions. Integration of multiple specialized packages, namely, MATLAB for image processing, R for statistical analysis, and ArcGIS for displaying and manipulating geospatial data, are adopted to unleash complex solutions that will practically benefit the rail industry and transportation researchers.

2 INTRODUCTION

The majority of rail accidents are attributed to train derailments, leading to operational shutdowns, financial losses, injuries, and even fatalities. A derailment takes place when a rolling stock becomes unstable and leaves its rail tracks resulting from a number of causes. These include the mechanical failure of turnout components, such as a worn or broken turnout frog or crossing nose. In the prediction analysis of these components, GIS and Mathematical modelling of assumptions are often employed. Compared to GIS, which became an option for analysing rail accidents at the beginning of 2000s, mathematical modelling of accidents is quite mature in transportation engineering.

The earliest example on a comprehensive mathematical study of railway accident rates was conducted by (Nayak, et al.) in 1983. The study deals with holistic derailment frequency and the probability distribution of the number of wagons and locomotives in the US. Its estimation methodology has been updated throughout several later studies with more sophisticated and specific methodologies. A quantitative correlation between derailment rate and track class has been

discovered which considers rail traffic and the location and frequency of derailments (Treichel & Barkan, 1993). Another study has enabled the probabilities of Class I and non-Class I railroad freight train accidents to be determined in a more precise way for the various classes of main-line track (Anderson & Barkan , 2004). Critical parameters have been revealed by utilising the US Federal Railroad Administration (FRA) accident database and related literature, then analysed in order to predict derailments of rolling stocks (Xiang , et al., 2011). The same research group (2017) also considers the FRA track class, method of operation, and annual traffic density in order to develop point estimators of and confidence intervals for derailment rates. Dindar et al. (2017) develops a Bayesian mathematical model with which to identify the risks of derailments caused by extreme weather conditions. The fundamental congruency between these studies on estimates of the derailment rates is a comprehensive methodology which is used to estimate various kinds of failures causing derailments. As train safety and risk analysis relies on accurate assessment of derailment likelihood, the more precisely the number of derailments across the region is estimated, the less maintenance expenses might be achieved, and the higher rail safety is provided within the region.

GIS has often been a preferred method for ensuring the higher rail safety , and identifying a weighted combination of the cost and risk associated with derailments for a set of reasons. The cost–risk trade-offs for railway shipments of hazardous materials has been studied in order to reveal some rerouting problems by overlaying the rail network on a census area map using GIS techniques (Glickman, et al., 2007). A quantitative risk analysis of hazardous materials, based on GIS, has been introduced to evaluate tank car design, product characteristics, traffic volume, infrastructure quality, and population exposure along shipment routes (Kawprasert & Barkan , 2010). Optimal frequencies for annual inspections of different track segments has also been developed by using GIS to determine accurately the route information for each rolling stock (Liu, 2017). Further, the impact of climate elements on component failures at rail turnouts (RTs or so-called ‘switches and crossings’) has been investigated by using GIS to calculate the exposure compounds (Dindar, Under review).

In general, mathematical models involved in the methodology of quantitative risk research might be accompanied by assumptions, some more heuristic than others. The characteristics of the data, e.g., correlational trends, distributions, and variable types, are, in general, determined by these assumptions. In railway risk research, many researchers have made various assumptions, particularly assumptions related to a set of risk indicators, i.e., rail traffic, in order to duplicate the intended research scenarios as closely as possible (Ishak, et al., 2016; Dindar, et al., 2017). The assumptions have been made on the basis of statistical data which corresponds to the studies up to a point. Therefore, the population, statistical tests used, research design, or other delimitations in the studies are highly likely to create uncertainties in readers.

This study investigates to what degree such frequently made assumptions, regardless of the GIS techniques used, impact the expected results. In order to do so, a region is segmented while taking climate conditions into account, which is aimed at eliminating the impact of climate. In order to analyse particular derailments related to component failures at railway turnouts, exposure levels of each state within the segmented region are determined by means of real data and/or a set of assumptions. Finally, using a comparison of the outcomes for different exposure levels, the derailment rates are eventually reached through a hierarchical Bayesian model (HBM).

3 DATA RELIABILITY AND USE

The US Department of Transportation authorises the FRA to conduct recordkeeping and report various kinds of accidents, i.e., derailments and collisions, under the regulations put forth in Title 49

of the Code of Federal Regulations (CFR) Part 22. The FRA uses these accident reports to identify comparative trends in railroad safety and develop risk reduction and hazard elimination programs associated with preventing railway injuries and accidents. One of the primary groups of accidents and incidents to be reported is rail equipment accidents/incidents. These groups will be coded throughout this study with a set of specific numbers.

This study investigates component failures at RTs, which are specified by the FRA codes T301 to T399. As shown in Table 1, the FRA discretises RT-related component failures into 18 types of accidents, each of which describes different failures at RTs and gives rise to various consequences.

Table 1 Reported Failures of Frogs, Switches, and Track Appliances at RTs

FRA Code	Description of failure
T301	Derail, defective
T302	Expansion joint failed or malfunctioned
T303	Guard rail loose/broken or mislocated
T304	Railroad crossing frog worn or broken
T307	Spring/power switch mechanism malfunction
T308	Stock rail worn, broken, or disconnected
T309	Switch (hand-operated) stand mechanism broken, loose, or worn
T310	Switch connecting or operating rod is broken or defective
T311	Switch damaged or out of adjustment
T312	Switch lug/crank broken
T313	Switch out of adjustment because of insufficient rail anchoring
T314	Switch point worn or broken
T315	Switch rod worn, bent, broken, or disconnected
T316	Turnout frog (rigid) worn or broken
T317	Turnout frog (self-guarded) worn or broken

T318	Turnout frog (spring) worn or broken
T319	Switch point gapped (between switch point and stock rail)
T399	Other frog, switch, and track appliance defect

RTs are known to be affected considerably by environmental conditions, i.e., temperature (Dindar, et al., 2016; Sa'adin, et al., 2016). As a result, physical changes in turnout components are expected to vary from a climate region to another. Therefore, it is suggested that regional segmentation on the basis of climatic characteristics might yield better estimation (Dindar, et al., 2017; Dindar, et al., 2017; Dindar, Under review). As the study intends to investigate the impact of assumptions on the results, the elimination of the additional impact of the climate itself could be necessary. Figure 1 shows the distribution of the climate zones across the US.

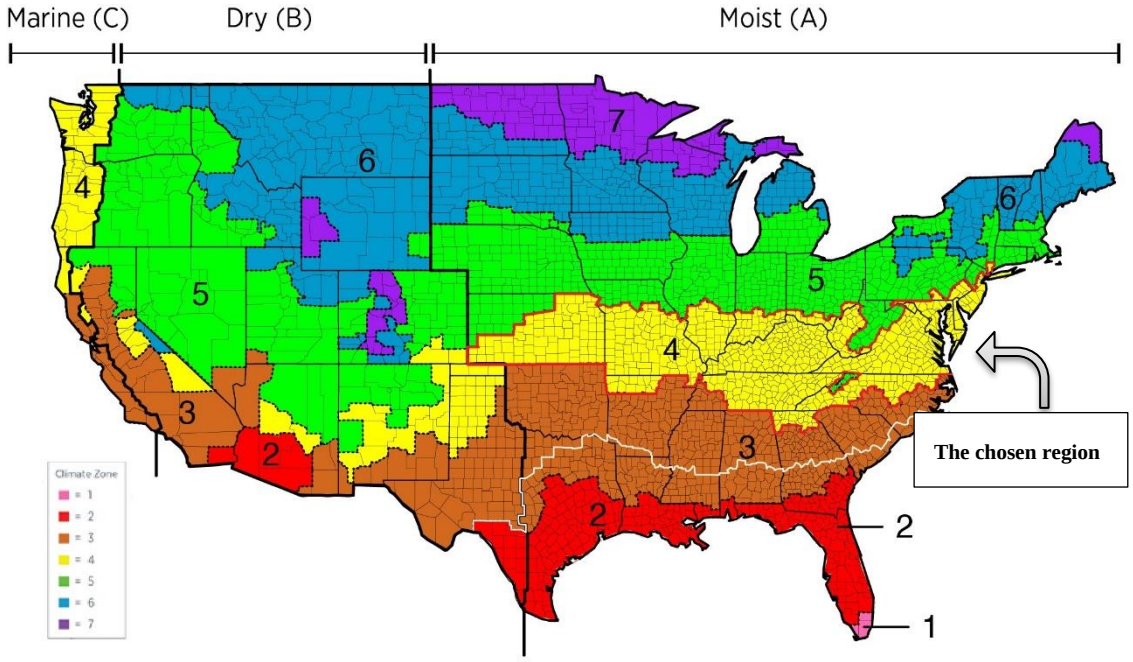

Figure 1 Climate Zones in the US

The US consists of seven fundamental, temperature-based zones (TBZs) and three precipitation-based zones (PBZs). The TBZs are numbered from 1 to 7, while the PBZs are divided into three groups, namely A to C. Each zone has unique variables, including precipitation, temperature, traffic density, and an intersectional variable, track class. This study will use a region composed of TBZ 4 and PBZ A, which is shown in yellow, outlined in red, and positioned to the right in Figure 1. Again, the reason for choosing this particular region is to minimise the impact of climate. The following states are included in the chosen region: Arkansas (AR), the District of Columbia (DC), Delaware (DE), Georgia (GA), Illinois (IL), Indiana (IN), Kansas (KS), Kentucky (KY), Missouri (MO), Maryland (MD), North Carolina (NC), New Jersey (NJ), New York (NY), Ohio (OH), Pennsylvania (PA), Tennessee (TN), Virginia (VA), and West Virginia (WV).

With approximately 140,000 miles of track in total US rail service as part of the interstate railway system, the FRA and US railway operators together undertake a full monitoring of the system's condition. All track is categorized into six classes, which indicate the quality of the track and are segregated by maximum speed limits. This study will concentrate on derailment estimates and severity on a state-by-state basis for entire networks in the chosen region. It is assumed that the condition of the turnouts is distributed homogenously through the states, as the study only focuses on derailments on entire tracks. However, the number of homogenously distributed turnouts in a state is said to be relevant to either the length of the railway network or the density of traffic (rail ton-miles per track mile per year[1]). Although the former would yield unrealistic results by considering the possibility of different counts of turnouts due to a large network, this paper leans towards the use of both the former and letter, which better offer reasonable information on to what degree turnouts on the entire network have exposure to any kind of rolling stock even under assumptions. Aside from the rail traffic measure in this region, the number of turnouts is assumed to be homogenously distributed. It is deterministically identified that there is one turnout[2] per 1.18 track mile (see Section 4.4.2) [17].

Regarding real data of density of traffic, a conventional method for measuring the rail traffic over a rail section, used mostly by the rail industry, is MGT, which is found by using ArcGIS. As this paper only focuses on turnouts (or 'switches and crossings'), the traffic over a turnout (instead of a section of rail) is used to calculate MGT-based rail traffic. Therefore, the measure of the MGT of traffic is based on the cumulative total static weight (including rail cars and locomotive or locomotives) of the traffic passing over a turnout within a year. MGT will be used as a unit of real data and as an assumption, which leads to a direct comparison between real data and mathematically-generated data. On the other hand, the measure of carloads, which is only used for an assumption, is obtained by counting the number of car which pass through carrying goods. In addition to carloads, rail ton-mile is also used to assume exposure to segmented regions, posing as the entire chosen region . This is another unit of rail traffic and is the equivalent of shipping one ton of product per one mile without considering any other kind of static weight, such as those of the locomotive and car. Both rail ton-mile and carloads will be compared to MGT in order to see how the estimation of derailment counts is achieved approximately through them.

4 METHEDOLOGY

4.1 Structure

The outline of the work is illustrated in Figure 2, which is composed of three technical phases. The overall aim is firstly to obtain derailment rates, by using different data sources, through different mathematical modelling techniques. Secondly, a comparable statistical analysis is achieved to benchmark the obtained derailment rates.

[1] This is the product of the annual total weight (including the weight of locomotives and loaded/unloaded wagons) and the distance moved by a rolling stock.

[2] The number of turnouts is determined only considering the number of switches in a rail section. For instance, a single crossover, consisting two switches, is described as two turnouts positioned in two tracks.

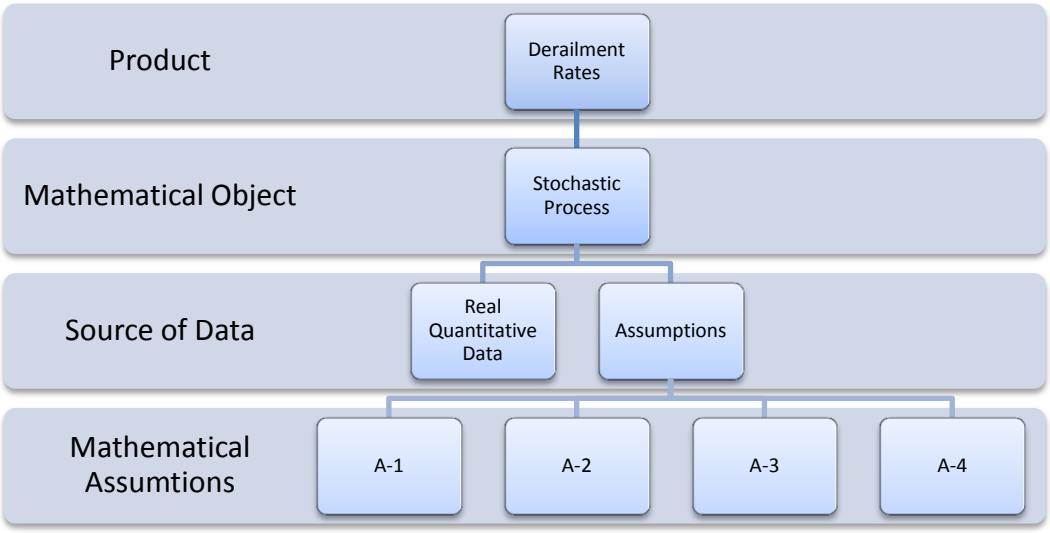

Figure 2 Phases of the Research

In order to fulfil a critical role in the achievement of the research objectives, stochastic process as a mathematical object is used. This is a novel mathematical process used to identify the distribution of the derailment rates at a given time with random variables, in contrast to a deterministic process built on derailment counts, rail traffic, and the number of rail turnouts. Data sources, i.e., real quantitative data (RQD) and assumptions, are outlined throughout the subsections below. The first three mathematical assumptions (A-1, A-2, and A-3) are associated with different units of rail traffic (million gross tonnes (MGT), rail ton-mile, and carloads, respectively), and the other assumption (A-4) refers to the number of turnouts, which is another risk indicator.

4.2 Engineering Assumptions

4.2.1 Exposure Indicators

In order to exclude environmental factors, the segmentation of the states is executed in accordance with climate patterns. As the density of the rail traffic and the number of rail turnouts within all of the segmented states are considered when investigating the number of derailments, both are considered to be exposure indicators in this study. To be more precise, the traffic density of a railway network influences considerably train safety and risk analysis and thereby leads to fluctuations in derailment rates. On the other hand, the more turnouts a rail network within the region possesses, the higher the expected number of derailments at turnouts.

It should be noted that the number of derailments is associated with some metric of traffic exposure indicators, such as car-miles, train-miles, gross ton-miles, or rail tonnes (Dindar, et al., 2016). As described in Section 3, MGT, carloads, and train-miles are presumed to be associated with the derailment of freight trains in this study.

Table 2 Normalised Exposure of RTs to Derailments in the Selected Region

	Illinois	Kansas	Nebraska	North Dakota	Oregon	Texas
TND	57	25	16	2	2	78
AATV	503.1	344.6	511.1	128.1	54.4	373.4
TRMS	6,986	4,855	3,375	3,330	2,396	10,469
NED	3,514,657	1,673,033	1,724,963	426,573	130,342	3,909,125

Table 2 shows various statistical patterns and risk indicators, e.g., the normalised exposure to derailment (NED). To obtain such a normalised exposure, the average annual traffic volumes (millions of tons) (AATV) of states might be presented as the first indicator of derailments. On the other hand, the number of RTs in a particular state is assumed, on average, in accordance with the values of TRMS (Total Rail Miles by State). That is, the number of turnouts might be correlated with the length of the rail network which a state possesses. The NED has been investigated through the product of these two indicators, AATV and TRMS. The total number of derailments (TND) is also seen to be a logical response to the output of this product.

It is worth noting that other sets of circumstances, e.g., weather conditions, speed, vehicle type, maintenance level, and time frame, have some effects on turnout-related derailments. However, the chosen region provides a useful, simplified way of reducing the effects of those indicators. Firstly, the region has the same weather characteristics throughout, and, secondly, might be considered to be quite large enough to exhibit a homogenous distribution of vehicle type over the given five-year period. It is important to keep in mind that derailments caused by speeding have been placed in another group of causes in FRA reports and that this study only focuses on turnout component failures that account for major causes of the turnouts-related derailments.

4.2.2 Assumptions on Indicators

The applied traffic pattern in the model, which will be identified later, might be expressed either in terms of a conventional method for measuring the traffic over a section of track used in the rail operation (MGT) or in terms of the number of wagons passing by, carloads. To be precise, the latter is the cumulative total of the static load over a section of engaged track, while the former is associated with the quantity of rolling stocks passing through a given section of rail track without considering how much weight is transported.

As indicators for a unit of rail traffic and the number of turnouts are investigated in order to comprehend their impacts on derailment rates, the following assumptions are necessary:

- A-1: as will be shown in Section 4.2.3., MGT traffic values contributed by each state to the given region (see Fig. 1) are calculated based on this assumption that the distribution of the MGT traffic values is homogeneous throughout the states.
- A-2: the rail ton-miles contributed by each state to the given region (see Fig. 1) are calculated assuming that the distribution of rail-ton miles is homogeneous throughout the states.

- A-3: the process established by A-1 & 2 is followed; however, the carload values are analysed as a traffic indicator instead and their distribution is assumed to be homogeneous throughout the states.

On the other hand, the number of turnouts, another exposure indicator, uses:

- A-4: a flowchart, suggested in Figure 2, is applied to distribute the number of turnouts across the chosen region. The length of rail network is assumed to be associated with the number of turnouts.

The data for the calculations for A1- A3 is obtained from the Association of American Railroads (AAC, n.d.). This source is only used for these three assumptions. At first glance, such assumptions might not be expected to help yield derailment rates. However, one of the aims of this study is the identification of which indicator yields better rates under given circumstances.

4.2.3 Area Calculation for the Regions

Seven US climate regions have been introduced and outlined in Section 3. In accordance with the different climate regions in Figure 1, different coloured layers are used for forecasting the expected relation between natural phenomena and railway component failures. In order to reveal this, a new mathematical model will be essential to the stochastic model establishment (see Eq-2 and Eq-3).

This subsection will investigate what proportions of the states identified in Section 4.2.1 fall into the chosen region. Image processing is firstly conducted through MATLAB. Although image processing has become popular in railway engineering, the applications have been limited to remote sensing (Dindar, et al., 2017). Thus, this paper, might be said to be following a different approach by using it to consider regional exposure to the risk of derailment.

The framework for the segmentation and quantification of the states is illustrated in Figure 3. The first phase in this framework is the input image, which projects the climate regions on the states, as shown in Figure 1. The input image includes black lines used to distinguish all of the regions, states and some counties from each other. Those black lines are then removed and filled in equally with the two neighbour colours. Then, a set of masking techniques are performed through the MATLAB toolbox, as illustrated in Figure 4.

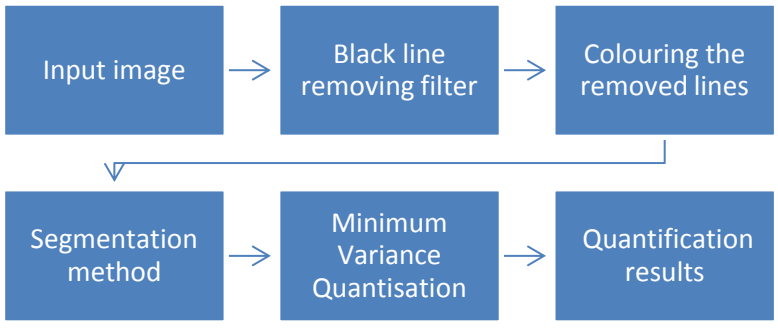

Figure 3 Flowchart of the Framework for the Quantification of the Climate Zones

In the fifth step, known as Rgb2ind[3], the maximum number of colours is specified in the output image's colormap to perform a minimum variance quantization. The numbers are selected to determine the number of boxes into which the RGB colour cube (R, G, B) indexed image (consisting of 255 colours) is separated. As result, the areas of all climate zones along with the test states are reached, and the findings are presented in Table 3.

Table 3 Quantification Results for the Climate Zones

Climate zones	Colour	Decimal Code (R, G, B)[4, 5]	Pixel Count	Proportion of sizes
1	Pink	(255, 105, 182)	500	0.001
2	Red	(255, 0, 0)	27,575	0.051
3	Brown	(210, 105, 33)	116,157	0.214
4	Yellow	(255,255,0)	48,369	0.089
5	Green	(0,245,0)	169,511	0.312
6	Blue	(0,155,205)	144,744	0.266
7	Purple	(0, 155, 240)	37505	0.069

Using an Intel ® Core™ i7 -6700 HQ processor, it took approximately 35 minutes to execute 2,000,000 pixels within the image through MATLAB.

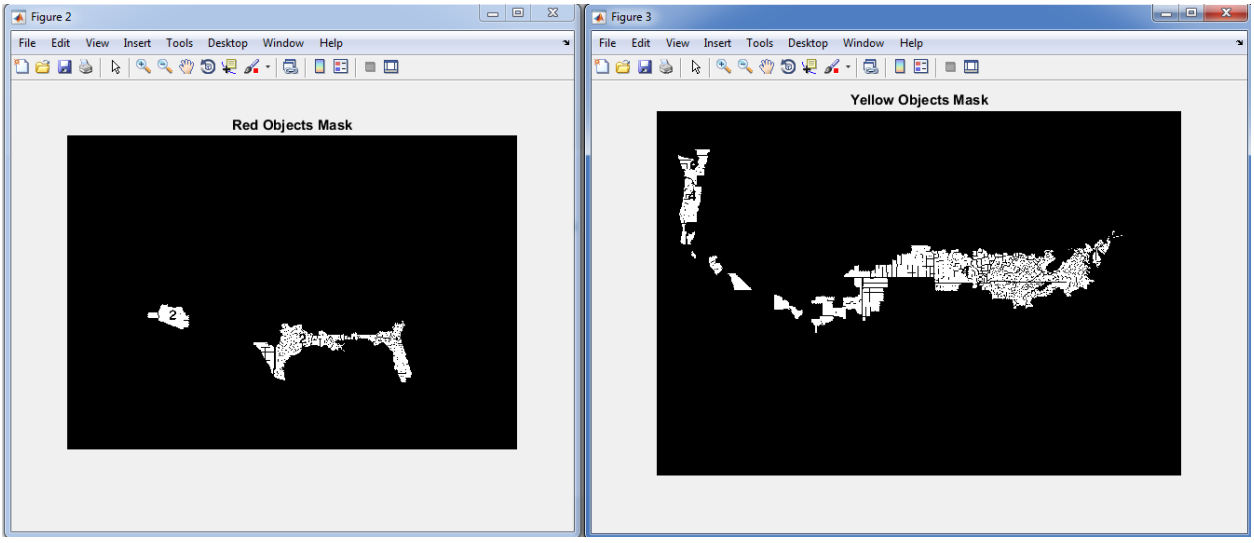

Figure 4 Area Segmentation Samples for Climate Regions

[3] a MATLAB function which converts the RGB image into an indexed image X using minimum variance quantization and dithering.

[4] The RGB values in the column are extracted from the image, which means that any value might only be addressed with the corresponding colour in the proposed map.

[5] The RGB values are coded within an interval of plus-and-minus 5.

4.3 Identification of Risk Exposure Indication Combinations

In order to better understand the effect of the new mathematical modelling on the risk exposure by rail transport to derailment, this study is designed to assess the performance of various assumptions against real data. Therefore, combinations of assumptions (traffic units and turnout counts) are required in order to perform the investigation. Figure 5 illustrates the entire structure to which the research has been applied. Dotted lines in the structure are used to express that only one box in the branch is utilised as an information source, whereas straight lines stress that mathematical equations, using all the data in the branch, are required to continue upward.

To clarify the figure in detail, the traffic indicator is selected among four data sources, namely, A-1 to 3, and RQD_{td}[6], while either A-4 or RQD_{tc}[7] is used as an additional data source. Throughout Eq-2 (see Section 4.4), the exposures of segmented regions are calculated with the chosen data source. Derailment estimates, then, are calculated using the exposures and real derailment counts by means of Eq-5 (see Section 4.4.). Therefore, as the selections of two different kinds of indicators within the two sets in which order is regraded are matched, eight combinations of two indicators can be drawn from these two indicator sets: RQD_{td} and RQD_{tc} (R_1), RQD_{td} and A-4 (X_1), A-1 and RQD_{tc} (X_2), A-1 and A-4 (X_3), A-2 and RQD_{tc} (X_4), A-2 and A-4 (X_5), A-3 and RQD_{tc} (X_6), and A-3 and A-4 (X_7).

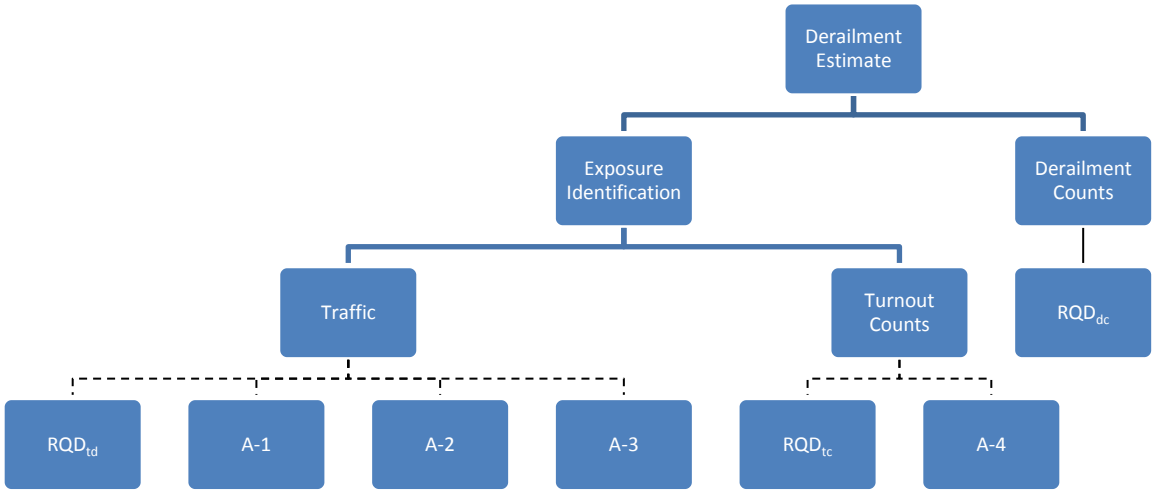

Figure 5 Structure for the use of the Assumptions and Real Database

[6] Real quantitative data for rail traffic density.

[7] Real quantitative data for turnout count.

4.4 Comparable Model Development

To conduct an analysis on the component failure rates at RTs and understand the precision of the mathematical assumptions on risk exposures, it is necessary to appoint a novel stochastic model, which is capable of estimating the rates of the derailment accidents within the chosen zone as effectively as possible. The novel model is required to respond both to real exposure values (the number of turnouts and traffic volume) and the values created by a set of assumptions using inexact data.

The structure of the model, therefore, is composed of a fixed formula, which is capable of addressing various kinds of exposure. Hierarchical modelling has been suggested to precisely estimate derailment rates of component failures at RTs in a given region (Dindar, et al., 2019). The modification of the suggested model (Albert, 1988) is illustrated in Eq.1.

$$p(\alpha,\mu|data) = \kappa \frac{z}{\Gamma^6(\propto)\ (\propto +z)^2 \mu} \sum_{i=1}^{18} \left(\frac{(\propto \text{ ^ } \propto\ \ \mu\text{^}(-\propto)\ \ \Gamma(\alpha+\ \lambda)}{(\propto/\ \mu+\ \pi\ )\text{^}((\propto\ +\lambda)} \right) \quad (1)$$

where α and μ are hyperparameters of a gamma function, κ is a proportionality constant, and i indicates state i within the chosen region. The verification of the model had been achieved (Albert, 1999). Thus, it can be identified that the marginal posterior density of (α, μ) id discovered through the suggested equation. Also, as the chosen region is made up of proportions from 18 different states, i= 1, …, 18. That is, each state contributes unequally to the marginal probabilities. Further, an MCMC algorithm is used to find a kernel density estimate of the simulated draws from the marginal posterior distribution (Albert, 1996).

In addition, π in Eq.1 is found by

$$\pi_i = \mathrm{e}_i \,.\, \lambda_i, \quad (2)$$

where λ denotes the occurrence rate in a given state (A-1, A-2 or A-3), and e (A-4) is the exposure (per year). The mathematical formula for the exposure is shown below.

$$\mathrm{e}_i\ = \sum_{i}^{18} w_i \,.\, TRMS_i.\,\mathrm{AATV}_{\,i}\,,\ \ i = 1,\ldots,18,\ \ \forall\, i\ \in \mathbb{N}, \quad (3)$$

where w_i is the proportion of the area corresponding to ith state in the assigned climate, i= 1, …, 18. For instance, if a quarter of the area that a state possesses falls into the chosen region, then w_i is 0.25.

$$\lambda_i = \sum_{i}^{18} w_i \,.\, \lambda_i \;, \qquad i = 1, \ldots, 18 \;, \;\; \forall\, i \;\in \mathbb{N} \;, \tag{4}$$

where $\lambda_i$represents occurrence rate for the proportion of ith state situated on the region. The acquisition of the occurrence rate (λ) corresponding to the chosen region follows a process equivalent to that used for the acquisition of the exposure (e). That is, after determining a constant value of w_i for ith state, the values of e and λ associated with this state are found by using Eq-3 and Eq-4. In addition, Eq-3 and Eq-4 are used for the assumptions (see Section 4.1). Eq-1 through Eq-5 consist of the second level of the hierarchical model. The first level is then simplified in the following equation in order to obtain derailment rates which are sampling from a gamma (α, α/μ) distribution of the form.

$$g_1\,(\lambda|\,\propto_1, \mu) = \frac{1}{\propto_1\; \Gamma(\propto_1)} \left(\frac{\propto_1}{\mu}\right)^{\propto_1} exp(-\propto_1 \lambda/\mu), \quad \lambda \;\in\; [0, +\infty), \tag{5}$$

where $\propto_1$ is the prior parameter of an inverse gamma function with hyperparameter $\propto$ (Albert, 1999). On the other hand, the state with the smallest estimated derailment rate for each combination can be identified through the following formula:

$$E\left(\frac{derailment\ count + \propto_1}{\pi + \left(\frac{\propto_1}{\mu}\right)}\right) \tag{6}$$

5 RESULTS

To both understand the performance of the assumptions compared to the real database and analyse the impacts of the assumptions on estimation of turnout component failures , the proportion of each state within the region is firstly computed. Table 4 has been established by the methodology presented in Section 4.2.3. It exhibits the complete details of the observed data and prediction. The

mathematical modelling has then been expanded to include the other two units of rail traffic, namely, rail ton-miles and carloads. As observed, some prediction models underperform compared to the RQD. Some relatively small proportions of states in the region, such as the proportions from AR and NY, have assumptions which diverge from RQD, while the remaining states' assumptions, e.g. DC, DE, and NJ, do well for the most part. Regardless of either how large or small the proportions from the states are or how much rail traffic is present in the states, an assumption which is based on turnout counts seem to fluctuate widely.

Table 4 Derailment-Risk Indicators for the States Located in the Chosen Region.

	Rail Traffic				Turnout Counts	
	ArcGIS	**Predictions**			**ArcGIS**	**Predictions**
States	RQD_{td} (MGT)	A-1 (MGT)	A-2 (Rail ton-miles)	A-3 (Carload)	RQD_{tc}	A-4
Arkansas	701	4341	34	549527	66	969
The District of Columbia	320	320	32	584800	319	36
Delaware	438	478	17	310600	145	450
Georgia	3730	2099	24	531664	117	1090
Illinois	11549	18643	170	4035137	1272	4237
Indiana	5356	8809	91	2156692	989	2321
Kansas	50510	35102	231	4120533	2914	5862
Kentucky	20668	20678	252	4351700	1526	4694
Maryland	5144	4743	81	1879260	620	1234
Missouri	35543	33979	311	5944221	1703	5201
North Carolina	5037	5713	40	695750	590	2812
New Jersey	1294	1163	26	883979	645	1041
New York	40	339	1	35286	190	130
Ohio	4151	6333	37	848620	288	1228
Pennsylvania	1747	2016	15	340029	627	724
Tennessee	17143	15856	179	3242668	1243	3822
Virginia	17489	17486	159	2851607	1301	5786
West Virginia	9907	5899	85	1385896	464	1764
Total	190766	183996	1786	34747969	14697	43401

Based on the results shown in Table 1, any quick decision for estimation of the derailments might not be advisable. The maximum likelihood method (MLE), a method which determines values for the

parameters of a model, is used to reveal the impact of the states on derailment counts on logarithmic x-axis in Figure 6. That is, the objective herein is to estimate the turnout-related derailment rates per unit of unique exposure (λ) which each state has. Thus, the MLEs (y/π)[8] for the chosen states show obvious inconstancies through each combination of exposure indicators. In general, New Jersey, Pennsylvania, and Georgia can be considered to not be at high risk of derailments considering their low turnout counts and rail traffic. It is worth noting that changes in the log exposure (x-axis) cannot be compared as the unit of exposure indicators vary throughout the combinations. However, this kind of estimate is open for discussion, as derailment events at turnouts, in particular those caused by component failure, are rare[9]. To remedy such a situation as much as possible, a Bayesian estimate, based on prior knowledge of the derailment rates, is used as shown in Section 4.4. As shown in Figure 6, the fact that a number of MLEs are placed at a low scale might also be expressed as proof of the necessity of performing a hierarchical Bayesian analysis.

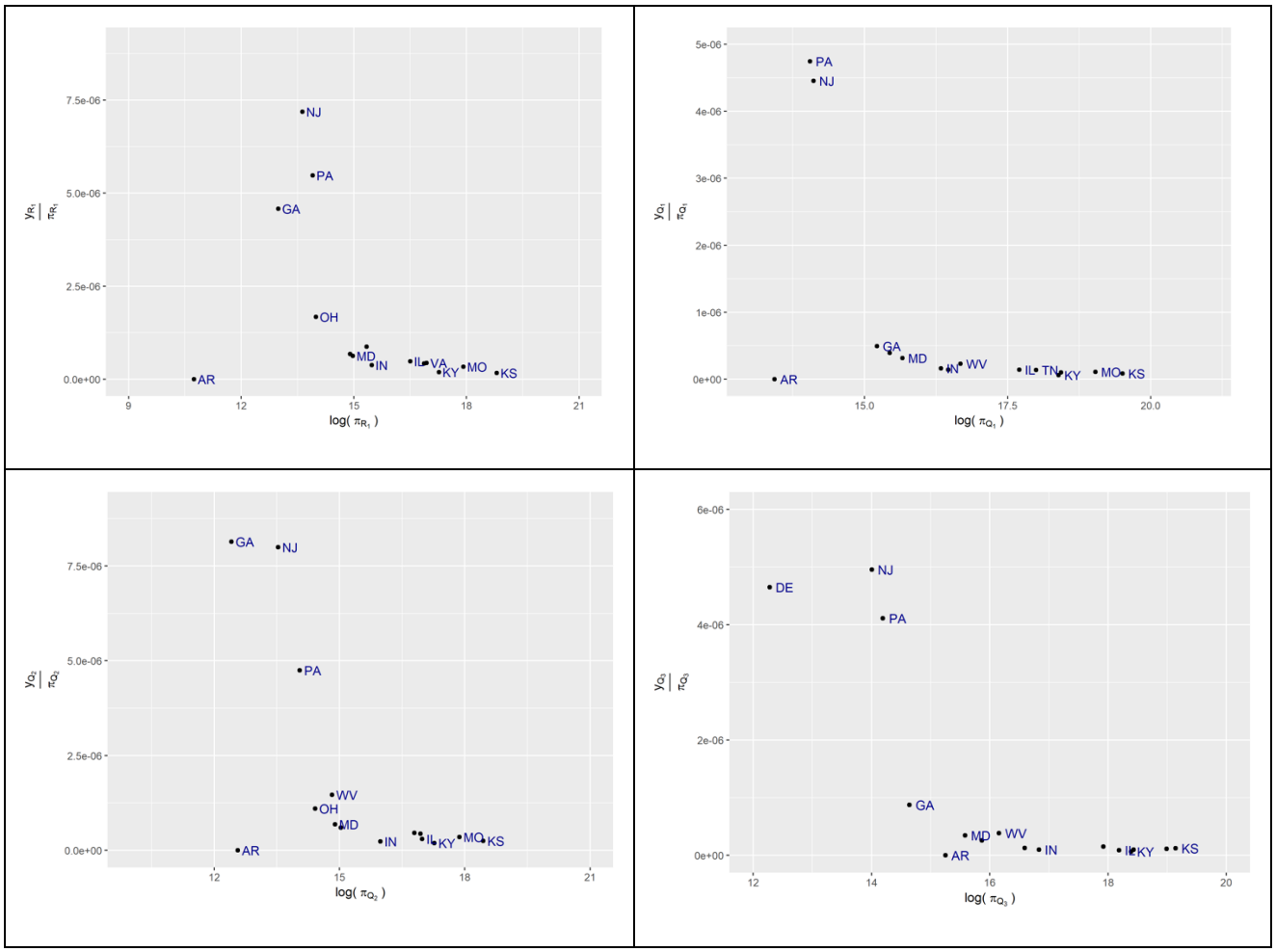

[8] The number of derailments per unit exposure

[9] Due to nature of MLE, as the number of derailments (y_i) becomes smaller, the estimate becomes worse. Moreover, if any derailment does not occur in a chosen region, it might still be quite unwise to bet that the estimate in question will never occur in the future.

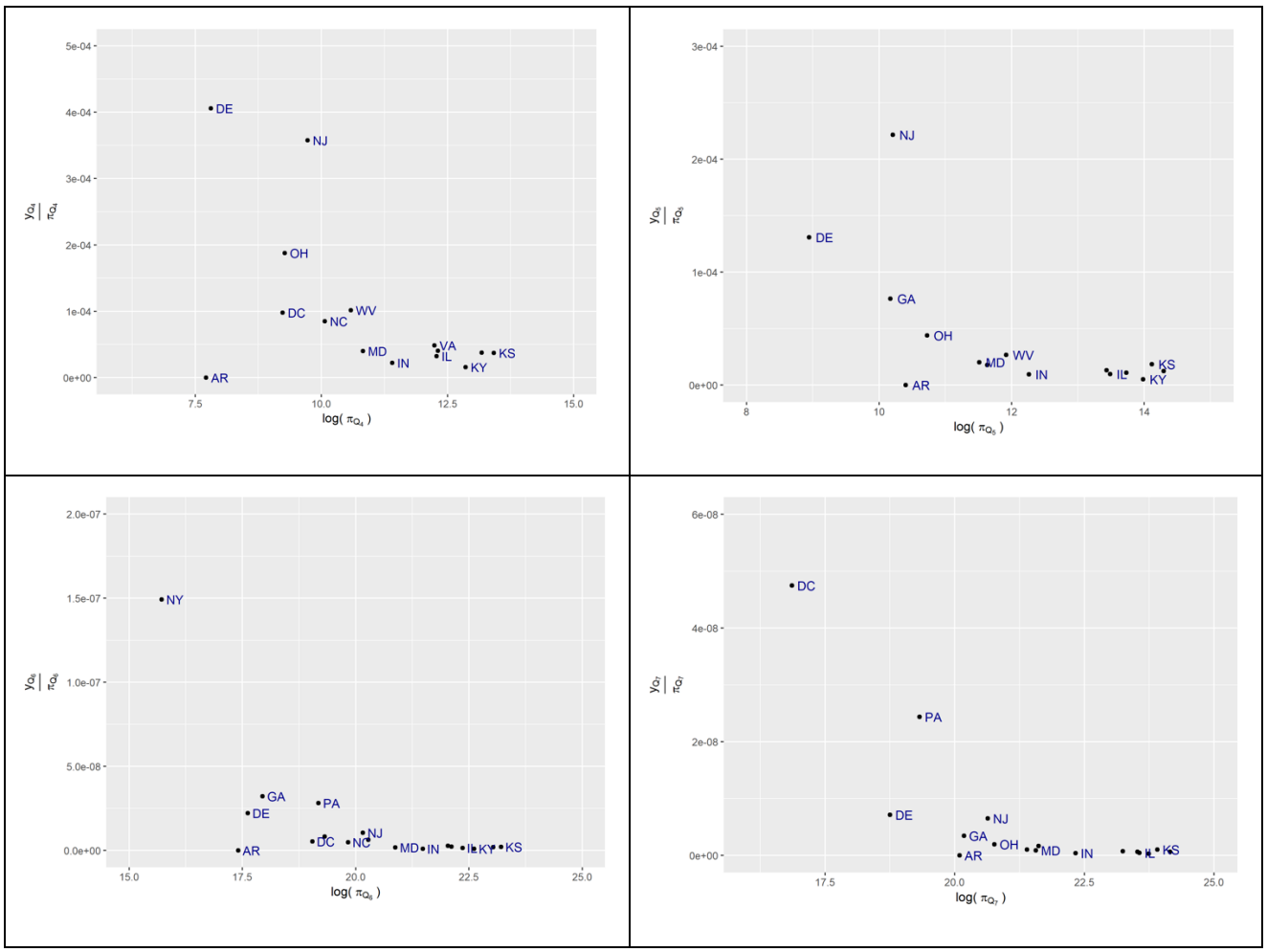

339 **Figure 6 MLE Estimates for the Chosen States**

340 Hyperparameters (α and μ), which are nested on the first floor of the structure (see Eq.5), must be
341 simulated using the marginal posterior distribution. It is noted that the posterior density for (log α,
342 log μ) is not shaped in a desired way. The normal approximation to the posterior, therefore, is
343 insufficient for proper simulation. Metropolis within the Gibbs algorithm[10] allows the log-
344 hyperparameters to be simulated. The initial trials in the simulation for the two conditional
345 distributions for each combination have been assigned the equivalent starting point (-5, -22). The
346 acceptance rates in the simulation are limited to 20%, and the number of iteration in the simulation is
347 50,000. Figure 7 illustrates the simulation trace plots for the assigned values of the hyperparameters
348 (α and μ) from the Bayesian hierarchical model.

[10] Available at https://www.rdocumentation.org/packages/LearnBayes/versions/2.15.1/topics/gibbs

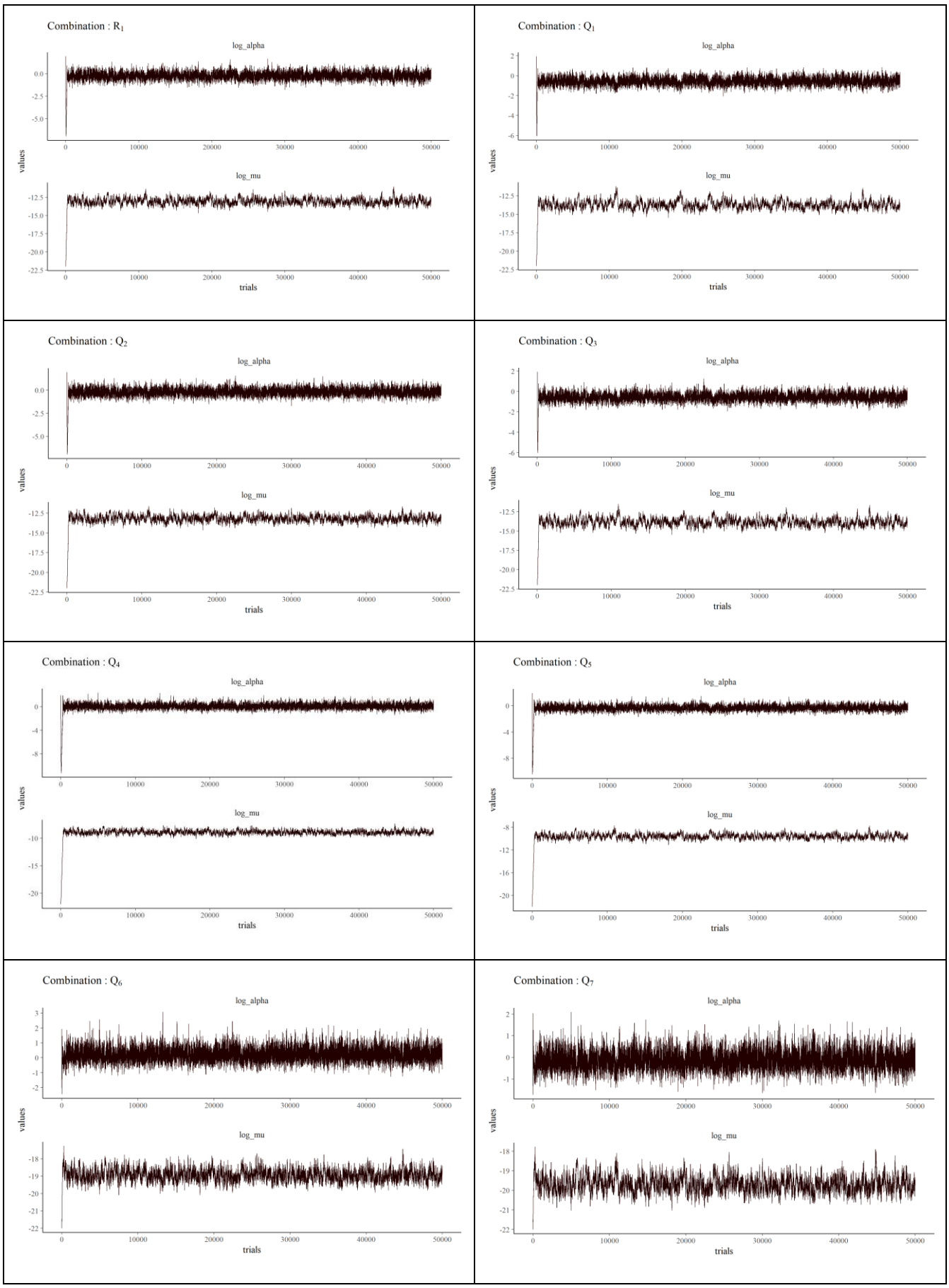
Combination : R_1
log_alpha
log_mu
values
trials
Combination : Q_1
log_alpha
log_mu
values
trials
Combination : Q_2
log_alpha
log_mu
values
trials
Combination : Q_3
log_alpha
log_mu
values
trials
Combination : Q_4
log_alpha
log_mu
values
trials
Combination : Q_5
log_alpha
log_mu
values
trials
Combination : Q_6
log_alpha
log_mu
values
trials
Combination : Q_7
log_alpha
log_mu
values
trials

Figure 7 Trace Plots of the MCMC Sampling Procedure for the combinations of log(α) and log(μ)

As seen in the traces for the combinations Q6 and Q7 (fully formed by assumptions) in Figure 7, there are wide fluctuations present, likely as derailment exposure indicators show inconsistency through the states.

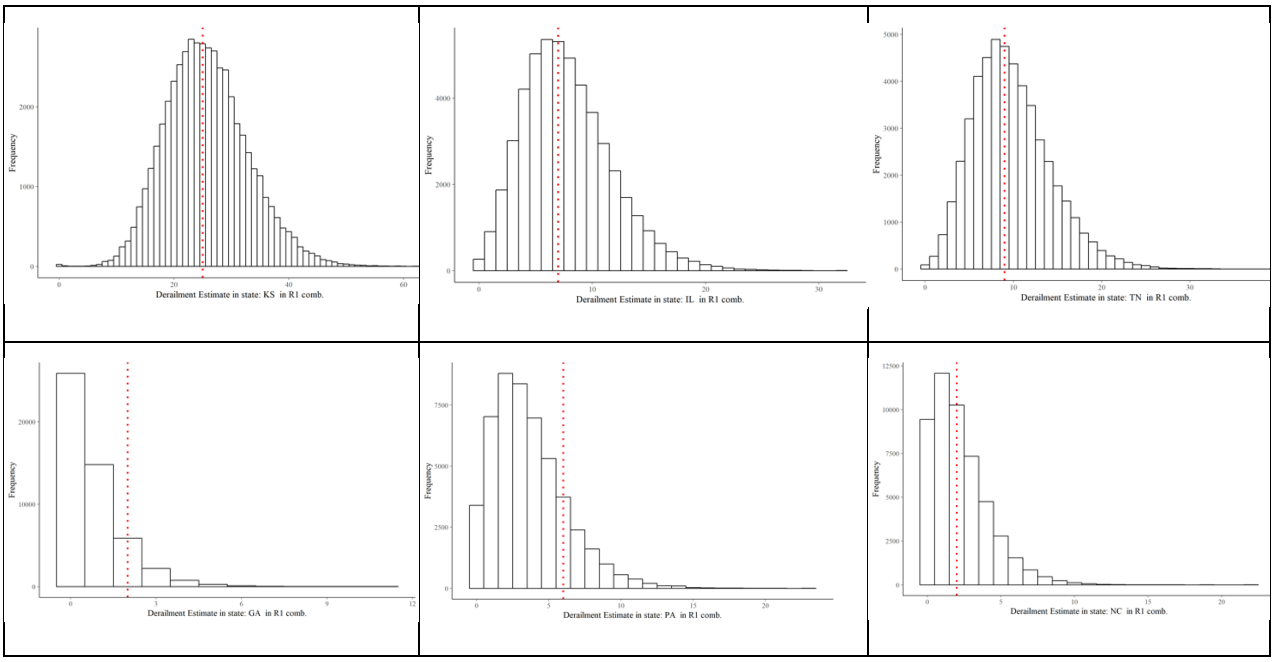

Figure 8 The number of Observed Derailments (red dotted line) and Histograms of the Simulated Draws from the Posterior Predictive Distribution for Several States for R1

The more symmetric the simulated draws on the right and left tails of the number of observed derailments are, the better the estimate. For instance, the first three histograms in Figure 8 indicate the robustness of the hierarchical model, while the distribution for GA does not. However, the estimate is seen to deviate slightly in regions with low numbers of derailments, which does not affect substantially the number of derailments in population, as the entire region has 107 derailment cases.

Table 5 Descriptive Statistics for the Bayesian Hierarchical Model Assigned with Various Exposures for the New York Rail Network[11]

	Min	Q_1	μ_{NY}	Q_3	Max	σ_{NY}	W^-	W^+	$\hat{p}_1$	$\hat{p}_{0,1,2}$

11 Min and Max: the minimum and maximum intensity values at the histogram, respectively.

Q1 and Q3: the values that cut off the first 25% and 75%, respectively, of the data when it is sorted in ascending order.

σ_i : standard deviation of derailment probability values for given ith state.

W^- *and* W^+ : a confidence interval for a proportion in a statistical population of derailment probability values

$\hat{p}_i$: the proportion of the point estimate for the actual count of the reported derailments to the whole

$\hat{p}_{i-1,\ i,\ i+1}$: the proportion of the point estimate for the actual observation along with the two nearest estimations to the whole

$R1_{NY}$	0	0	0.03432	0	3	0.1902179	0.02994607	0.03300592	0.03144	0.99998
$X1_{NY}$	0	0	0.02144	0	4	0.151726	0.01859588	0.0210379	0.01978	0.99994
$X2_{NY}$	0	0	0.238	0	6	0.5387683	0.1560788	0.1624935	0.15926	0.9931
$X3_{NY}$	0	0	0.1455	0	5	0.4181237	0.1039449	0.1093555	0.10662	0.99726
$X4_{NY}$	0	0	0.0512	0	3	0.2308671	0.0450225	0.04872713	0.04684	0.99988
$X5_{NY}$	0	0	0.02758	0	5	0.1710553	0.02421271	0.02698019	0.02556	0.99994
$X6_{NY}$	0	0	0.07128	0	3	0.2727648	0.06186831	0.06615868	0.06398	0.99997
$X7_{NY}$	0	0	0.03484	0	3	0.1908583	0.03070778	0.03380409	0.03222	0.99994

Table 5, for instance, shows some statistical outcomes of simulated draws for New York Rail Network, which has a low number of derailments (Y_{NY} =1). Probing μ_{NY} (mean of the draws) and σ_{NY} (standard deviation of the draws), all of the combinations are said to be clustered around 0, which is not desired, as one derailment is reported in the region. Therefore, the actual coverage probability close to the nominal value of (W^-, W^+) is satisfying. However, as this particular derailment case is rarely observed, the point estimate for the actual count of the reported derailments, $\hat{p}_1$, is extended with the probability of zero derailments or two derailments $\hat{p}_{0,1,2}$. As expected, $R1_{NY}$ yields the best outcome with a probability of 0.99998. The other combinations, however, are not poor estimates.

Table 6 Descriptive Statistics for the Bayesian Hierarchical Model Assigned with Various Exposures for the Illinois Rail Network

	Min	Q_1	μ_{IL}	Q_3	Max	σ_{IL}	W^-	W^+	$\hat{p}_1$	$\hat{p}_{6,7,8}$
$R1_{IL}$	0	5	7.592	10	32	3.919311	0.1012163	0.1065646	0.10386	0.30908
$X1_{IL}$	0	5	7.511	10	30	3.86311	0.1021653	0.1075354	0.10482	0.32068
$X2_{IL}$	0	5	7.705	10	34	3.907449	0.1046964	0.1101239	0.10738	0.32260
$X3_{IL}$	0	5	7.517	10	33	3.852057	0.1043998	0.1098206	0.10708	0.32424
$X4_{IL}$	0	5	7.792	10	32	3.919311	0.1035692	0.1089713	0.10624	0.31970

$X5_{IL}$	0	5	7.604	10	39	3.894708	0.1027783	0.1081624	0.10544	0.32190
$X6_{IL}$	0	5	7.972	10	32	3.940043	0.1017303	0.1070905	0.10438	0.31486
$X7_{IL}$	0	5	7.741	10	35	3.920828	0.1043800	0.1098004	0.10706	0.32066

Considering the regions, which are expected to have higher derailment rates, Tables 6 and 7 illustrate the statistical outcomes of the given combinations. X7, which is made up of two assumptions (A-3 and A-4) and X6, which is made up of real data and an assumption (RQD and A-4), yields the worst estimates. Derailment rates in Kansas, which has one of the largest rail networks and the heaviest rail traffic in the chosen region, show that the $\hat{p}_1$ and $\hat{p}_{24,25,26}$ values, in particular for X6 and X7, deviate by 25 percent in comparison with R1.

Table 7 Descriptive Statistics for the Bayesian Hierarchical Model Assigned with Various Exposures to the Kansas Rail Network

	Min	Q_1	μ_{KS}	Q_3	Max	σ_{KS}	W^-	W^+	$\hat{p}_1$	$\hat{p}_{24,25,26}$
$R1_{KS}$	0	21	25.84	30	74	7.176168	0.05486403	0.05892406	0.05686	0.16744
$X1_{KS}$	0	21	25.55	30	62	7.121259	0.05164026	0.05558833	0.05358	0.16118
$X2_{KS}$	0	21	25.73	30	70	7.164428	0.05486403	0.05892406	0.05686	0.16672
$X3_{KS}$	0	21	25.48	30	62	7.130782	0.05631929	0.06042857	0.05834	0.16706
$X4_{KS}$	0	21	25.71	30	63	7.146079	0.05382199	0.05784626	0.05580	0.16664
$X5_{KS}$	0	21	25.49	30	67	7.146889	0.05311430	0.05711406	0.05508	0.16970
$X6_{KS}$	0	21	25.8	30	62	7.163830	0.04832036	0.05214875	0.05020	0.14914
$X7_{KS}$	0	21	25.5	30	63	7.089469	0.04512061	0.0488290	0.04694	0.13756

6 DISCUSSION

A risk quantification based on a Bayesian hierarchical model is a novel technique for conducting safety analysis in railway engineering and gives rise to a huge potential in terms of railway applications across many engineering domains. This paper argues that there are differences in the

various mathematical assumptions used as risk indicators and uses both these and recorded observations in a derailment risk analysis which concentrates on component failures at RTs. The outcomes enable to be more precise derailment estimation, allowing for a concrete risk rail management. As a result, the potential for severe consequences is able to be minimized through better understanding the factors influencing train derailment associated with this kind of failures. This study; therefore, meets the need for the judgment of effectiveness and feasibility of assumptions, as one of the influencing factors. The proposed methodology uses a real dataset (obtained with ArcGIS) and three different assumptions (consisting of mathematical methods) for measuring the density of traffic over turnouts and one real dataset (obtained with ArcGIS) and one assumption (consisting of a mathematical method) for the number of derailments. To eliminate climate impact on derailment counts, a large enough region is determined by considering official climate reports. Eighteen states, each with a different level of risk exposure, are included in the region to be investigated. Their risk indicators, hence, risk exposures, are calculated throughout either using a real FRA database or mathematically-generated databases (assumptions) or a combination thereof. Then, the least to most risky three states are selected to consider the outcomes. Based on a well-established Bayesian hierarchical model, comparisons of the advantages and disadvantages between the use of real data and assumptions or combinations thereof are as follows:

- From the perspective of the regions with quite low risk indicators, e.g. NY, the assumptions yield derailment estimate rates around the actual observations in this region. However, all of the estimates seem to be incapable of calculating an estimate for a low number of derailments and are identified as the most sensitive estimates in such regions. The primary reason for this unreliable estimate by each combination is a scarce data environment within the risk indicators and low derailment counts. To overcome this, it might be suggested that the time period selected for derailment analysis be extended. Derailments, which occurred over the last five years, were taken into account in this study. As the number of derailments increases, the more precise outcomes should become. In other words, sampling should represent a subset of all data. To satisfy the sampling analysis, 50,000 derailment samples were generated, which seems to be enough to reach a conclusion, by considering the smooth distributions of bars in Figure 8. Onn the other hand, as such small regions do not impact concretely the estimate of the total number of derailments in the entire region, the cumulative number of derailments might be obtained in the desired fashion.

- From the perspective of the regions with moderate-risk indicators e.g. Illinois[12], it is determined that it is possible for a precise estimate of the derailment rates to be determined under any uncertainty, which might be formed by the assumptions. It is worth noting that this study is conducted on the basis of a hierarchical Bayesian model estimating the parameters of the posterior distribution of turnout-related derailments in two stages. By using this advanced technique, additional evidence on the prior distribution can be acquired. The technique allows for a novel prediction of the true derailment rates to the extent permitted by the input data. It is observed that any region with low risk indicators, e.g. the number of turnouts and freight traffic density, can be investigated with one of the suggested assumptions; namely A-1 to 4 (see Section 4.2.2).

[12]Illinois has actually quite high risk indicators. However, the area covered by Illinois in the chosen region is identified as posing a derailment risk lower which is lower than that of the entire state.

- From the perspective of the regions with high-risk indicators, e.g. Kansas, some of the assumptions, particularly those, which relied on turnout counts, are observed to deviate from the observations. In contrast to wanting a larger sample size in the first bullet, the larger sample sizes in the assumptions in this case generally lead to decreasing precision when estimating derailment rates. In other words, the decrease in precision for larger sample sizes is largely associated with minimal or even non-existent data. This might arise mainly from the presence of errors in the assumptions or a strong dependence in the real data. It could also be the result of better statistical results following a heavily-tailed (asymmetrical) distribution in such situations.

- From the perspective of assumption types, it can be identified that the assumptions regarding turnout counts are a weak spot even when being generated mathematically on the basis of a concrete belief. This study employs the proportion of turnout counts and rail-network length. As the EU countries are relatively more populated in comparison to the US, European rail networks thereby require a larger number of turnouts in a short rail section. In case of a paucity of reliable guidance on the estimation of the number of derailments in a given region, particularly with high exposure, the subjective judgment of an expert might be utilized before conducting the analyses. In order words, the study accepts that there is one turnout per 1.18 miles in this region of the US, even though this suggestion reflects a much higher number of turnouts than the US has. Moreover, demand for rail service stems from demands elsewhere in the economy for the products that railways haul. That is, each state has unique characteristics, which cause each one to build more or less of a rail network. Therefore, unique turnout numbers for such regions are needed, found using real data or an expert's judgment, to reach the saturation of the sample.

7 CONCLUDING REMARKS

To ensure a proper rail operation and achieve effectively safety goals, prevention of turnout-related derailment has been a topic of concern to railway operators and the general public. Derailment predictions for turnouts are typically obtained through highly complicated statistical analyses associated with large potential risks. In recent decades, increasing awareness in safety risk analysis and the management of rail networks has resulted in the necessity of calculating derailment probabilities, considering root causes, and determining which particular rail infrastructures are more or less exposed. This study focuses on component failure-related derailment at RTs. Considering the potential impact of climate on component failures, the study employs a large enough region in the US to investigate derailments without having to consider climatic variations.

The number of new suggestions for prediction of train derailment at RTs is presented in this paper. Based on engineering assumptions and observations, it can be identified that regions with a moderate occurrence of derailment rate yield congruent results regardless of whether the data resource is based on rational assumptions or real data. Also, the most vulnerable assumption is determined to be turnout counts. Subject-matter expert judgement is suggested for the integration of an such assumption in future failure analysis in railway engineering as well as in other congruent railway infrastructures.

The success of the land segmentation, on the other hand, can be underlined. The impact of climate on rail infrastructure failures is a well-known phenomenon. As this study segmented land area by state, a well-performing methodological structure is established, enabling the climate impact to be

eliminated. The suggested methodology for derailment estimates is observed to have the ability to overcome the complexity of the prediction of derailment in the segmented region.

8 ACKNOWLEDGEMENT

The authors would like to thank British Department for Transport (DfT) for Transport - Technology Research Innovations Grant Scheme, Project No. RCS15/0233; and the BRIDGE Grant (provided by University of Birmingham and the University of Illinois at Urbana Champaign). The first author gratefully acknowledges Turkish Ministry of Education for supporting his PhD at University of Birmingham. The authors are sincerely grateful to the European Commission for the financial sponsorship of the H2020-RISE Project No. 691135 "RISEN: Rail Infrastructure Systems Engineering Network", which enables a global research network that tackles the grand challenge of railway infrastructure resilience and advanced sensing in extreme environments (www.risen2rail.eu).

9 Bibliography

AAC, n.d. *Association of American Railroads.* [Online] Available at: https://www.aar.org/data-center/railroads-states/ [Accessed 12 01 2018].

Albert, J., 1988. Computational Methods Using a Bayesian Hierarchical Generalized Linear Model. *Journal of the American Statistical Association* , 83(404), pp. 1037-1044.

Albert, J., 1996. A MCMC algorithm to fit a general exchangeable model. *Communications in Statistics - Simulation and Computation*, 25(3).

Albert, J. H., 1999. Criticism of a hierarchical model using Bayes factors. *Statistics inMedicine*, 18(3), pp. 287-305.

Anderson, R. & Barkan , C., 2004. Railroad Accident Rates for Use in Transportation Risk Analysis. *Transportation Research Record: Journal of the Transportation Research Board,* Volume 1863, pp. 88-98.

Dindar, S. & Kaewunruen, S., 2017. Assessment of Turnout-Related Derailments by Various Causes. In: J. G. Pombo J., ed. *Recent Developments in Railway Track and Transportation Engineering.* Cham: Springer, pp. 27-39.

Dindar, S., Kaewunruen, S. & An, M., 2016. Identification of appropriate risk analysis techniques for railway turnout systems. *Journal of Risk Research.*

Dindar, S., Kaewunruen, S. & An, M., 2017. Derailment-based Fault Tree Analysis on Risk Management of Railway Turnout Systems. *Materials Science and Engineering,* 245(4).

Dindar, S., Kaewunruen, S. & An, M., 2019. A Bayesian-based hierarchical model for analysis of climate on hazardous rail component failures.

Dindar, S., Kaewunruen, S., An, M. & Barrera, Á.-G., 2017. *Derailment-based Fault Tree Analysis on Risk Management of Railway Turnout Systems.* Prague, s.n.

514 Dindar, S., Kaewunruen, S., An, M. & Osman, M., 2016. Natural hazard risks on railway turnout
515 systems. *Procedia engineering,* Volume 161, pp. 1254-1259.

516 Dindar, S., Kaewunruen, S., An, M. & Sussman, J., 2017. Bayesian Network-based probability
517 analysis of train derailments caused by various extreme weather patterns on railway turnouts. *Safety*
518 *Science,* Issue In Press.

519 Dindar, S., Kaewunruen, S. & Osman, M. H., 2017. *Review On Feasibility of Using Satellite Imaging*
520 *for Risk Management of Derailment Related Turnout Component Failures.* Prague, IOP Conf. Series:
521 Materials Science and Engineering, p. 245.

522 Dindar, S., Kaewunruen, S. & Osman, M. H., 2017. Review On Feasibility of Using Satellite
523 Imaging for Risk Management of Derailment Related Turnout Component Failures. *IOP Conference*
524 *Series: Materials Science and Engineering,* 245(4).

525 Dindar, S., Kaewunruen, S. & Sussman, J. M., 2017. Climate Change Adaptation for GeoRisks
526 Mitigation of Railway Turnout Systems. *Procedia engineering,* Volume 189, pp. 199-206.

527 Dindar, S., Under review. Hierarchical Modelling of Derailment-causing Component Failures for
528 Railway Turnouts: An Inverse Gamma-Poisson based Bayesian Prediction..

529 Gelman, A., 2006. *Prior distributions for variance parameters in hierarchical models.* Volume 1,
530 Number 3, pp. 515–533: Bayesian Analysis.

531 Glickman, T. S., Erkut, E. & Zschockec, M. S., 2007. The cost and risk impacts of rerouting railroad
532 shipments of hazardous materials. *Accident Analysis & Prevention,* 5(39), pp. 1015-1025.

533 Gustafson, P., Hossain, S. & Macnab, Y., 2003. Conservative prior distributions for variance
534 parameters in hierarchical models. *The Canadian Journal of Statistics,* Volume 31.

535 Ishak, M. F., Dindar, S. & Kaewunruen, S., 2016. *Safety-based maintenance for geometry restoration*
536 *of railway turnout systems in various operational environments.* Songkhla, Thailand, s.n.

537 Kawprasert , A. & Barkan , C., 2010. Communication and Interpretation of Results of Route Risk
538 Analyses of Hazardous Materials Transportation by Railroad. *Transportation Research Record:*
539 *Journal of the Transportation Research Board.*

540 Liu, X., 2017. Optimizing rail defect inspection frequency to reduce the risk of hazardous materials
541 transportation by rail. *Journal of Loss Prevention in the Process Industries,* Volume 48, pp. 151-161.

542 Nayak, P. R., Rosenfield, D. B. & Hagopian, J. H., 1983. *Event probabilities and impact zones for*
543 *hazardous materials accidents on railroads,* Washinghton D.C: U.S. Department of Transportation.

544 Sa'adin, S. L. B., Kaewunruen, S., Jaroszweski, D. & Dindar, S., 2016. *Operational risks of*
545 *Malaysia-Singapore high speed rail infrastructure to extreme climate conditions.* ART-2016, Jeju,
546 Korea, The 1st Asian Conference on Railway Infrastructure and Transportation.

547 Treichel, T. T. & Barkan, C. P., 1993. *Working Paper on Mainline Freight Train Accident Rates,*
548 Washington, D.C: Research and Test Department, Association of American Railroads.

549 Xiang , L., Barkan, C. & Rapik, S. M., 2011. Analysis of Derailments by Accident Cause Evaluating
550 Railroad Track Upgrades to Reduce Transportation Risk. *Transportation Research Record,* Issue
551 2261, pp. 178-185.

552 Xiang , L., Saat , R. M. & Barkan, C. .. P., 2017. Freight-train derailment rates for railroad safety and
553 risk analysis. *Accident Analysis and Prevention,* Issue 98, pp. 1-9.

554

555